This paper is available on line at http://www.mcponline.org

# Increased Protein Nitration in Mitochondrial Diseases: Evidence for Vessel Wall Involvement

**Gaetano Vattemi‡, Yehia Mechref§, Matteo Marini‡, Paola Tonin‡, Pietro Minuz¶, Laura Grigoli‡, Valeria Guglielmi‡, Iveta Klouckova§, Cristiano Chiamulera‖, Alessandra Meneguzzi¶, Marzia Di Chio‖, Vincenzo Tedesco‖, Laura Lovato‡, Maurizio Degan¶, Guido Arcaro¶, Alessandro Lechi¶, Milos V. Novotny§, and Giuliano Tomelleri‡‡**

**Mitochondrial diseases (MD) are heterogeneous disorders because of impairment of respiratory chain function leading to oxidative stress. We hypothesized that in MD the vascular endothelium may be affected by increased oxidative/nitrative stress causing a reduction of nitric oxide availability. We therefore, investigated the pathobiology of vasculature in MD patients by assaying the presence of 3-nitrotyrosine in muscle biopsies followed by the proteomic identification of proteins which undergo tyrosine nitration. We then measured the flow-mediated vasodilatation as a proof of altered nitric oxide generation/bioactivity. Here, we show that 3-nitrotyrosine staining is specifically located in the small vessels of muscle tissue and that the reaction is stronger and more evident in a significant percentage of vessels from MD patients as compared with controls. Eleven specific proteins which are nitrated under pathological conditions were identified; most of them are involved in energy metabolism and are located mainly in mitochondria. In MD patients the flow-mediated vasodilatation was reduced whereas baseline arterial diameters, blood flow velocity and endothelium-independent vasodilatation were similar to controls. The present results provide evidence that in MD the vessel wall is a target of increased oxidative/nitrative stress.** ***Molecular & Cellular Proteomics 10: 10.1074/mcp.M110.002964, 1–10, 2011.***

Mitochondrial diseases (MD)[1] are heterogeneous disorders because of impairment of respiratory chain function, causing defective mitochondrial energy production (1, 2). Respiratory chain is under dual genetic control, the mitochondrial DNA (mtDNA) and nuclear DNA; the clinical phenotype, when associated with mtDNA mutations, largely depends on the degree of mitochondrial heteroplasmy in high energy requiring tissues, primarily skeletal and cardiac muscle and central nervous system, and on the biochemical expression of mtDNA abnormalities (1, 2). MD are responsible for about 1% of all the cases of diabetes mellitus (3) and, as regards neuromuscular disorders, there is an estimated prevalence of one case per 5000 in the general population (1). Two major metabolic abnormalities may derive from mtDNA mutations: impaired energetic metabolism and increased oxidative stress (4). Reduced ATP generation, from both uncoupling of electron transport and decreased synthesis from ADP by mitochondrial ATP synthase, decreases the availability of energy supply generated through the tricarboxylic acid circle (4). Oxidative stress may be increased in cells harboring a mtDNA mutation that causes faulty electron transport and generation of radical oxygen species, which, in turn, induce an overexpression of antioxidant enzymes (4–7).

The present investigation was aimed at exploring whether the vessel wall is affected in mitochondrial respiratory chain disorders and whether increased oxidative/nitrative stress is causally involved. Our working hypothesis was that reactive nitrogen species (RNS), including peroxynitrite ($ONOO^-$) and nitrogen dioxide ($^{\bullet}NO_2$), were the eventual fate of endothelium-derived nitric oxide (NO) in the setting of MD (8). The crucial role of endothelial cells in the maintenance of vascular homeostasis is strictly related to their capability to generate and release biologically active NO (9, 10). Mitochondrial dysfunction may alter NO bioactivity through increased ROS production and generation of highly RNS, particularly peroxynitrite, via the fast diffusion-controlled reaction with superoxide

From the ‡Department of Neurological Sciences and Vision, Section of Clinical Neurology, University of Verona, Italy, §Department of Chemistry, Indiana University, Bloomington, Indiana, 47405, ¶Department of Biomedical and Surgical Sciences, Section of Internal Medicine, University of Verona, Italy, and ‖Department of Medicine and Public Health, Section of Pharmacology, University of Verona, Verona, Italy

Received July 9, 2010, and in revised form, November 17, 2010

Published, MCP Papers in Press, December 12, 2010, DOI 10.1074/mcp.M110.002964

[1] The abbreviations used are: MD, mitochondrial diseases; mtDNA, mitochondrial DNA; RNS, reactive nitrogen species; NO, nitric oxide; 3-NT, 3-nitrotyrosine; FMD, flow-mediated vasodilatation; nNOS, neuronal ntric oxide synthase; eNOS, endothelial NOS; iNOS, inducible NOS; UEA-I, *Ulex europaeus* agglutinin-I; CFA, common femoral artery.

TABLE I

*Characteristics of patient population. MERRF: myoclonic epilepsy with ragged red fibers; MELAS: mitochondrial encephalomyopathy with lactic acidosis and stroke-like episodes; MIDD: maternally inherited diabetes and deafness; CPEO: chronic progressive external ophthalmoplegia*

| Patient | Sex | Age (years) | Age at onset | Clinical phenotype | mtDNA mutation |
|---|---|---|---|---|---|
| 1 | M | 44 | 40 | MERRF | A8344G |
| 2 | M | 53 | 47 | MERRF | A8344G |
| 3 | M | 46 | 36 | MERRF | A8344G |
| 4 | M | 42 | 41 | MELAS | A3243G |
| 5 | M | 30 | 18 | MELAS | A3243G |
| 6 | M | 53 | 35 | MELAS | A3243G |
| 7 | M | 16 | 6 | MELAS | A3243G |
| 8 | M | 38 | 37 | MIDD | A3243G |
| 9 | F | 50 | 46 | CPEO | Single deletion |
| 10 | M | 59 | 53 | CPEO | Single deletion |
| 11 | F | 67 | 54 | CPEO | Single deletion |
| 12 | M | 35 | 33 | Mitochondrial myopathy | Not yet identified |
| 13 | F | 57 | 54 | Mitochondrial myopathy | Not yet identified |
| 14 | M | 40 | 36 | Mitochondrial myopathy | Not yet identified |
| 15 | M | 64 | 62 | Mitochondrial myopathy | Not yet identified |
| 16 | M | 53 | 50 | Mitochondrial myopathy[a] | Not yet identified |

[a] Mitochondrial myopathy and diabetes mellitus.

(11, 12). A hallmark of these nitrogen species is the conversion of tyrosine to 3-nitrotyrosine (3-NT), whether free or part of a polypeptide chain (11, 12). This nitration of tyrosine can compromise the functional and/or structural integrity of target proteins (13–15).

We investigated the pathobiology of vasculature in MD first, by assaying the presence of 3-NT in muscle biopsies followed by the proteomic identification of proteins that undergo tyrosine nitration, and then, by measuring the flow-mediated vasodilatation (FMD) as a proof of altered NO generation/bioactivity.

## EXPERIMENTAL PROCEDURES

*Patients*—Available muscle biopsy specimens from 16 patients with mitochondrial respiratory chain dysfunction were evaluated; the same patients were then recalled and invited to participate in this study. The characteristics of our patient population are summarized in Table I. The clinical diagnosis was based on established criteria (16). mtDNA abnormalities were identified in 11 patients; 3 had myoclonic epilepsy with ragged-red fibers (MERRF) and the A8344G mutation, 4 had mitochondrial encephalomyopathy with lactic acidosis and stroke like episodes (MELAS) and the A3243G mutation, 1 had maternally inherited diabetes and deafness (MIDD) and the A3243G mutation, and 3 had chronic progressive external ophthalmoplegia (CPEO) and a single deletion. Two patients (patient 15 and 16) had histological [ragged red fibers (RRFs) and cytochrome *c* oxidase (COX) deficiency] and biochemical (complex IV deficiency) signs of mitochondrial myopathy; three patients had morphological signs of mitochondrial myopathy (patient 12 had 5% of RRFs and COX deficiency in 20% of the fibers; patient 13 had subsarcolemmal mitochondrial accumulations in 3% of the fibers and COX deficiency in 10% of the fibers; patient 14 had 3% of RRFs). In these five patients, affected with a proximal myopathy (patient 16 had also diabetes mellitus), mtDNA mutations have not been identified yet.

Patients were pair matched for gender, diabetes mellitus, and cigarette smoking, with 16 nonaffected subjects. The two patients and two control subjects who were moderate cigarette smokers (10 cigarettes/day) were invited to refrain from smoking on the study days. All the subjects gave their informed consent to be included in the study that was approved by the Internal Reviewing Board of our Institution.

*Histology and Histochemistry*—Muscle samples were snap frozen in liquid nitrogen-cooled isopentane. Serial 8-$\mu$m-thick cryosections were stained with hematoxylin and eosin, modified Gomori trichrome, ATPase (pH 4.3, 4.6, and 10.4), succinate dehydrogenase (SDH), cytochrome *c* oxidase (COX), NADH-TR, Periodic Acid Schiff, Sudan black, and acid phosphatase.

*Immunohistochemistry and Confocal Immunofluorescence Microscopy*—Immunohistochemical studies were performed on 6.5-$\mu$m-thick transverse muscle sections using fluorescence method with a well-characterized rabbit polyclonal antibody to 3-NT (Upstate Biotechnology). Immunohistochemistry for neuronal nitric oxide synthase (nNOS), endothelial NOS (eNOS), and inducible NOS (iNOS) was also done on serial 6.5-$\mu$m-thick cryosections. Postcutting fixation was not done on sections. Controls were muscle biopsies from subjects who were ultimately deemed to be free from muscle diseases.

Double immunofluorescence was performed using antibody to 3-NT and eNOS in combination with (a) a mouse monoclonal antibody to smooth muscle actin, as a marker of vascular smooth muscle cells and (b) a biotinylated *Ulex europaeus* agglutinin-I (UEA-I), as an endothelial cell marker. The reaction was examined by confocal fluorescence microscope (LSM510, Zeiss).

To control staining specificity the primary antibody was omitted or replaced with nonimmune sera at the same concentration. Two independent, blinded investigators evaluated the relative staining.

*Quantification of 3-Nitrotyrosine-positive Blood Vessels*—For quantification studies, double immunofluorescence was performed with antibody to 3-NT in combination with biotinylated UEA-I, as described. The total number of blood vessels and the number of 3-NT-positive blood vessels were quantitatively analyzed in biopsy specimens from seven patients (2, 5, 7, 8, 10, 13, and 15) and 75 controls. The comparison of the relative staining was carried out by two independent, blinded investigators.

*Measurement of eNOS-positive Vessel Wall*—For quantification studies, digital photomicrographs of eNOS-positive blood vessels were acquired and analyzed using the NIH Scion Image analysis program in biopsy specimens from seven patients (see previous section) and seven controls that were matched for age, sex, and biopsied muscle. The total area of the vessel wall and the area of the eNOS-positive vessel wall were blindly measured for each subject

($n$ = 2–9 slides/subject). The ratio between the eNOS immunoreactive area and the total area was obtained for each vessel wall by dividing these values.

*Assay of NOS Activity*—NOS activity assay was performed by measuring ($^3$H) L-arginine (Amersham Biosciences) to ($^3$H) L-citrulline conversion with a NOS assay kit (Cayman Chemicals, Ann Arbor, MI) according to the manufacturer's instructions. Muscle biopsies from eight patients (2, 5, 7, 8, 9, 10, 13, and 15) and 11 controls who were matched for age, sex and biopsied muscle were evaluated. All measurements of NOS activity were normalized for total proteins. Protein concentration was determined with the Bradford method.

Muscle tissue was homogenized with a lysis buffer (Tris-HCl 25 mM, EDTA 1 mM, EGTA 1 mM). For the nNOS and eNOS determination the supernatants were incubated for 60 min at 37 °C in a reaction buffer (Tris-HCl 25 mM, tetrahydrobiopterin 3 $\mu$M, flavin adenite mononucleotide 1 $\mu$M, flavin adenite dinucleotide 1 $\mu$M), and in the presence of NADPH 10 mM, ($^3$H) L-arginine 50$\mu$Ci/$\mu$l, and $CaCl_2$ 6 mM. As the inducible isoform of NOS is calcium-independent, the determination of iNOS activity was performed in the absence of $CaCl_2$. The reaction was stopped with HEPES 50 mM, pH5.5 and EDTA 5 mM and the equilibrated resin, which specifically binds to arginine, was added to the sample reaction. Following centrifugation, $^3$H L-citrulline content in the eluate was quantified in a $\beta$-counter (Beckmann). Control reactions were performed with iNOS and nNOS positive controls and with L-MNNA for negative controls.

*SDS-PAGE Electrophoresis, Two-dimensional Gel Electrophoresis and Immunoblot Analysis*—The expression of nNOS and eNOS was evaluated by one-dimensional immunoblotting as described (17). Coomassie Blue staining was used to assess protein loading. Bands were quantified densitometrically using the Quantity One software (Bio-Rad).

The presence of nitrated proteins was investigated by two-dimensional immunoblot. For two-dimensional gel electrophoresis, frozen human muscle was homogenized in lysis buffer (7 M urea, 2 M thiourea, 4% w/v 3-[(3-cholamidopropyl)dimethylammonio]-1-propanesulfonic acid, 40 mM Tris-base, and 65 mM dithioerythritol). Protein load was 60 $\mu$g for analytical gels and 120 $\mu$g for gels to transfer. The IEF (first dimension) was carried out on nonlinear wide-range immobilized pH gradients (pH 3–10; 18 cm long IPG strips) and the second dimension on 6–18% T polyacrylamide linear gradient gels. Analytical gels were stained with ammonical silver nitrate. Gels to transfer were blotted on 0.2 $\mu$m nitrocellulose membranes (BioRad) for 16 h (Trans-Blot Cell; BioRad, Hercules, CA), and stained with 0.2% Ponceau S Red solution to sign on acetate sheets the references of protein migration and facilitate the computer-aided matching of silver stained gel. Two-dimensional immunoblots were performed using antibody to 3-NT. To reveal false immunopositive spots, the membrane was chemically reduced with a solution of 10 mM sodium dithionite in 50 mM pyridine acetate buffer, pH 5.0, for 1 h at room temperature, as described (18). Following reduction, the membrane was extensively washed with distilled water and probed with the antibody to 3-NT. The immunopositive spots detected following the reduction were not considered for further analysis. The two-dimensional gel and the two-dimensional immunoblot images were analyzed and matched with the Image Master two-dimensional Platinum v6.0 software (Amersham Biosciences). Briefly, immunopositive spots on the autoradiographic films were first matched with the Ponceau S references and then with two-dimensional reference map of analytical gel.

*Protein Identification*—Protein spots were excised from two-dimensional gels, destained in 25 mM ammonium bicarbonate, 40% ethanol, and washed with acetonitrile. Trypsin digestion was performed according to our previously published procedure (19). Briefly, gel pieces were placed in Eppendorf tubes and cut into smaller (less than 1 mm in each dimension) pieces. Gel pieces were covered with 200 $\mu$l of 200 mM ammonium bicarbonate buffer prepared in 40% acetonitrile and incubated at 37 °C for 30 min to destain spots. The solution was then removed from the tube and discarded. Next, gel pieces were completely dehydrated by drying in an Eppendorf Vacufuge concentrator (Brinkmann Instruments, Westbury, NY) for 20 mins. Twenty microliters of 20 $\mu$g/ml trypsin solution (in 36 mM ammonium bicarbonate, 9% acetonitrile) were then added to the dried gel pieces. After gel pieces were rehydrated, 50 $\mu$l of 40 mM ammonium bicarbonate prepared in 9% acetonitrile were added. Samples were incubated for 18 h at 37 °C prior to removing the liquid from gel pieces and transferring to a new prewashed tube. Trypsin digests (~70 $\mu$l) were dried in the Vacufuge concentrator and reconstituted in 10 $\mu$l of water. These solutions were immediately subjected to LC-MS/MS analysis.

Six microliters of trypsin digested gel pieces were loaded on a PepMap300 C18 cartridge (5 $\mu$m, 300 Å, Dionex, Sunnyvale, CA) then separated on an in-house packed 150 mm × 75 $\mu$m i.d. pulled-tip nano-column packed with C12 Jubitor Proteo-90 Å (Phenomenex, Torrance, CA). Sample elution was attained using a 15-min gradient from 100% to 65% solvent A, 97:3:0.1 water/acetonitrile/formic acid (solvent B was 0.1% formic acid in acetonitrile) at 250 nL/min using an Ultimate 3000 nano-LC system (Dionex, Sunnydale, CA). From the end of the column, ions were electrosprayed directly to an linear trap quadrupole (LTQ) FT mass spectrometer (ThermoElectron, San Jose, CA), which recorded mass spectra and data-dependent tandem mass spectra of the peptide ions. MSMS spectra were searched against protein sequences for *Homo sapiens* in the Swiss-Prot database using a licensed copy of MASCOT for peptide sequence determination and subsequent protein identification. A protein was reported to be found in a spot only when three or more peptides obtained a score at or above the "identity or extensive homology" score (95% confidence).

The score for an MS/MS match is based on the absolute probability ($P$) that the observed match between the experimental data and the database sequence is a random event. Ions score is $-10^*\text{Log}(P)$, where P is the probability that the observed match is a random event. Individual ions scores > 30 indicate identity or extensive homology ($p < 0.05$). Also, Expect which is the number of times we would expect to obtain an equal or higher score, purely by chance was employed. The lower this expectation value is, the more significant the results are.

Peak list was generated using our in-house developed software (TurboRAW2Mgf). This utility, described in details in Reference 20, is available as part of ProtQuant, which can be acquired freely from http://ncgg.indiana.edu. The parameters used to extract peaks in this utility are MW 600–45,000; absolute total ion intensity threshold 100; minimum ion count 5; retention time tolerance (min) 1; precursor tolerance (ppm) 20; and peak tolerance (ppm), 200. The peak list generated using this utility was searched using MASCOT 2.0 search engine employing trypsin as the enzyme with 2 possible missed cleavages. Because the samples were reduced and alkylated, carbamidomethyl fixed modification of cystine residues was used. No variable modification was used. Mass tolerance of precursor ion was set to 2 Da, whereas that of the fragment ion was set to 0.8 Da. Uniprot-sprot database released on September 10, 2008 was used with Homo sapiens subset of Uniprot-sprot which has 20328 sequences.

*Immunoprecipitation and Immunoblotting*—To validate the correct identification of nitrated proteins, immunoprecipitation of the putative modified proteins including vimentin, desmin, ATP synthase $\beta$-chain subunit, protein disulfide-isomerase A3, voltage-dependent anion channel 1 and MnSOD, and Western blotting with 3-NT antibody were performed. Briefly, frozen muscles were homogenized in lysis buffer (50 mM Tris-HCl, 150 mM NaCl, 1% Nonidet P-40, 0.1% SDS, 1 mM EDTA, 0.5% deoxycholic acid, pH 8.0, with protease inhibitors).

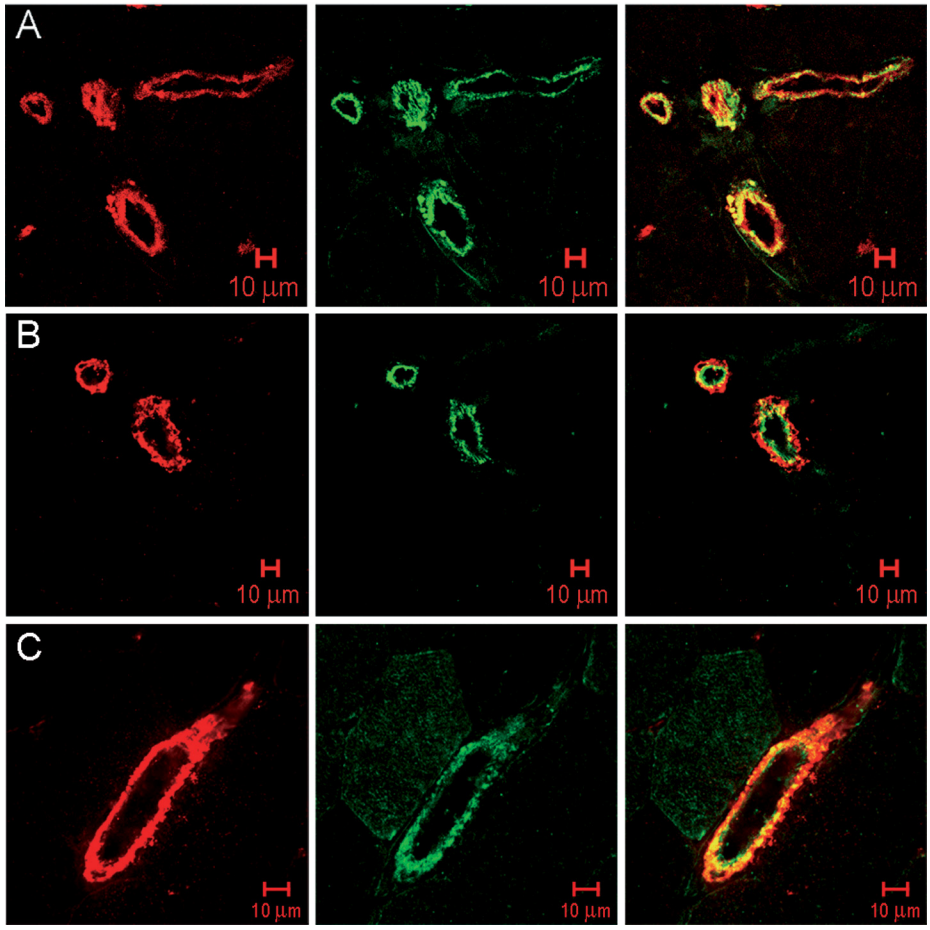


FIG. 1. **Confocal fluorescence microscopical images of 3-nitrotyrosine-positive blood vessels from a patient with mitochondrial disease.** *A*, Shows the localization of 3-nitrotyrosine (*green*) to endothelial cells, labeled with UEA-I (*red*). Capillaries do not stain with 3-nitrotyrosine. *B*, shows a partial colocalization of 3-nitrotyrosine (*green*) to smooth muscle cells, labeled with actin (*red*) whereas in panel *C* 3-nitrotyrosine is localized to almost all the smooth muscle cells of the vessel wall.

Aliquots corresponding to 0.5 mg of protein were first precleared by incubation with protein A-agarose (Roche Applied Science) for 1h at 4 °C and then incubated with the relevant antibody overnight at 4 °C on a orbital shaker. Protein A-agarose was added for 3 h at 4 °C and following centrifugation, the immunoprecipitated material was washed three times with lysis buffer. Following addition of two-dimensional buffer, proteins were resolved by two-dimensional-gel electrophoresis, blotted on nitrocellulose membrane, and then incubated with the antibody to 3-NT. Proteins were detected as previously described.

*Flow-mediated Vasodilatation and Echo-Doppler Analysis*—Endothelial function was investigated according to the model of FMD using a high-resolution ultrasound echo Doppler (Esaote AU5) with a 7,5 MHz linear transducer. The axial resolution of this probe was 0,05 mm and ultrasonic calipers accurate to 0,05. Each patient was investigated in a controlled environment at 22 °C. After patients rested for 15 min in the supine position, systolic, diastolic, mean blood pressure, and heart rate were determined every 2 min by an oscillometric recorder (Dinamap, model 845, Critikon, Tampa, FL) positioned on the right arm. To assess the basal values of each hemodynamic test, we considered the average of three blood pressure determinations and heart rate recordings. We measured common femoral (CFA) and brachial (BA) artery diameters and flow velocity at a fixed position: 1 cm before CFA bifurcation and 1 cm above the elbow fold. Hemodynamic measurements, related to FMD, were obtained 30 s and 1, 2, 4, 6, and 8 min after the beginning of distal hyperemia and were related to the flow velocity increase at the level of investigated arteries. Thirty minutes after, endothelium-independent vasodilatation (*i.e.* induced by a nitric oxide donor) was tested; changes in brachial and femoral artery diameter were recorded 3 and 5 min following the sublingual administration of nitroglycerin (300 $\mu$g).

Diameter variations were expressed as percentage of the basal diameter. The area under the curve was calculated with the trapezoidal method (21). Two observers carried out echo-doppler investigations and hemodynamic measurements.

Echo-Doppler analysis of the carotid arteries was performed to evaluate the presence of atherosclerotic lesions and the intima-media thickness.

*Statistical Analysis*—The $\chi$-square test was used for the comparisons of 3-NT in blood vessels of patients and controls. The Student's *t* test for unpaired comparison was used for ratio values of eNOS-positive vessel wall. One-way ANOVA was used to compare NOS activity in patients and controls. The Mann-Withney test was used to compare two variables in patients and controls when indicated. A *p* value of 5% or less was considered as statistically significant.

## RESULTS

*Immunohistochemistry and Confocal Fluorescence Microscopy*—Nitrotyrosine was detected in the wall of small blood vessels (inner diameter ranging from 5 to 100 $\mu$m), which were located within the interfascicular septa, from the patients' muscle biopsy whereas no staining was observed in the examined capillaries (Fig. 1). A partial colocalization of 3-NT was observed to endothelium (labeled with UEA-I), as well as to smooth muscle cells (labeled with actin) of blood vessels, (Fig. 1). 3-NT staining was stronger in the patients than in controls

TABLE II

*Quantification of 3-nitrotyrosine-positive (NT+) blood vessels. The total number of blood vessels and the number of 3-nitrotyrosine-positive (NT+) and 3-nitrotyrosine-negative (NT-) blood vessels were quantitatively analyzed in biopsy specimens from seven patients and seventy-five control subjects*

| Age (year) range | Patients | | | | | Controls | | | | | |
|---|---|---|---|---|---|---|---|---|---|---|---|
| | Subjects (n) | Total vessels (n) | NT+ vessels (n) | NT-vessels (n) | NT+ vessels (%) | Subjects (n) | Total vessels (n) | NT+ vessels (n) | NT-vessels (n) | NT+ vessels (%) | p value |
| 0–9 | | | | | | 8 | 174 | 6 | 168 | 3.4 | |
| 10–19 | 1 | 28 | 14 | 14 | 50.0 | 11 | 206 | 10 | 196 | 4.8 | <0.001 |
| 20–29 | | | | | | 11 | 207 | 10 | 197 | 4.8 | |
| 30–39 | 2 | 56 | 20 | 36 | 35.7 | 11 | 266 | 13 | 253 | 4.9 | <0.001 |
| 40–49 | | | | | | 11 | 287 | 37 | 250 | 12.9 | |
| 50–59 | 3 | 132 | 86 | 46 | 65.1 | 9 | 236 | 39 | 197 | 16.5 | <0.001 |
| 60–69 | 1 | 63 | 40 | 23 | 63.5 | 10 | 322 | 59 | 263 | 18.3 | <0.001 |
| >70 | | | | | | 4 | 117 | 40 | 77 | 34.2 | |

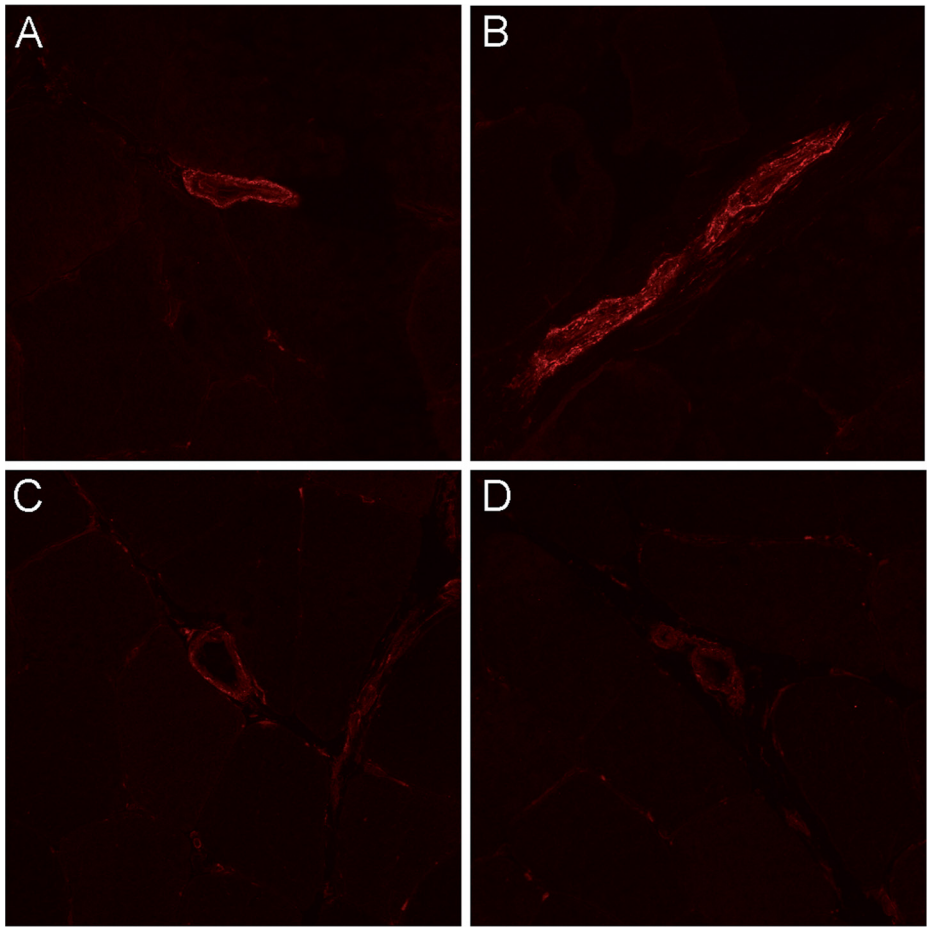


FIG. 2. **Immunofluorescence images of eNOS-positive blood vessels.** *A*, and *B*, showing the stronger staining for eNOS in the vessel wall from a patient with MELAS (patient 4) as compared with two pair-matched control subjects (*C*, and *D*).

and a quantitative analysis, performed in 7 out of 16 patients, showed that nitrotyrosine positive vessels were significantly different in patients and controls, thus providing evidence of increased RNS production (Table II). The striking data was the similar, or even higher, percentage of 3-NT positive vessels in the younger patients as compared with our controls over 70. In the oldest patients this percentage reached almost 65, three times more than what observed in aged-matched controls.

The nNOS immunoreactivity was restricted to the sarcolemma of the muscle fibers and the staining was comparable in patients and controls (data not shown).

Immunolabeling for eNOS was observed in the vessel wall from the patients' and controls' muscle biopsy. However, the staining was stronger in the patients than in controls (Fig. 2) and the image analysis of eNOS-positive blood vessels, performed in 7 out of 16 patients, revealed that the stained area for eNOS—expressed as the ratio of the eNOS immunoreac-

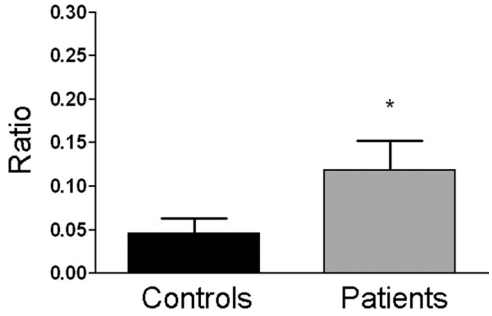


FIG. 3. **Measurement of eNOS-positive vessel wall.** Box plots show the ratio of the eNOS immunoreactive area out of the total area of each vessel in patients and controls. Data are from seven patients with mitochondrial diseases and seven pair-matched controls.

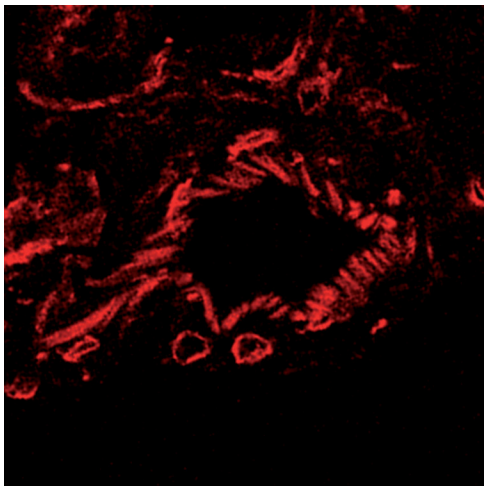

FIG. 4. **Immunofluorescence image of iNOS-positive blood vessel.** A blood vessel stained for iNOS from a patient with MELAS (patient 4).

tive area out of the total area of each vessel—was significantly higher in the patients than in controls (Fig. 3), thus suggesting an increased expression of the enzyme.

Immunostaining for iNOS largely produced no positive signal in either control or patient blood vessels. A positive staining for iNOS was seen in a few blood vessels from patients with MELAS (Fig. 4).

*SDS-PAGE Electrophoresis and Immunoblot Analysis*—By immunoblotting, eNOS was increased in the patients' muscles as compared with controls, whereas the expression of nNOS was similar in patient and control muscles (Fig. 5).

*Assay of NOS Activity*—Total NOS activity, the calcium-dependent activity of the constitutive isoforms of NOS (eNOS and nNOS) as well as the calcium-independent activity of iNOS, were increased in the patients' muscle biopsies compared with control muscles (Fig. 6). However, the differences were not statistically significant.

*Identification of Specific Nitrated Proteins in MD Patients*—By two-dimensional gel electrophoresis followed by immunoblot analysis with antibody to 3-nitrotyrosine, 11 immunoreactive spots were identified exclusively in the patients as compared

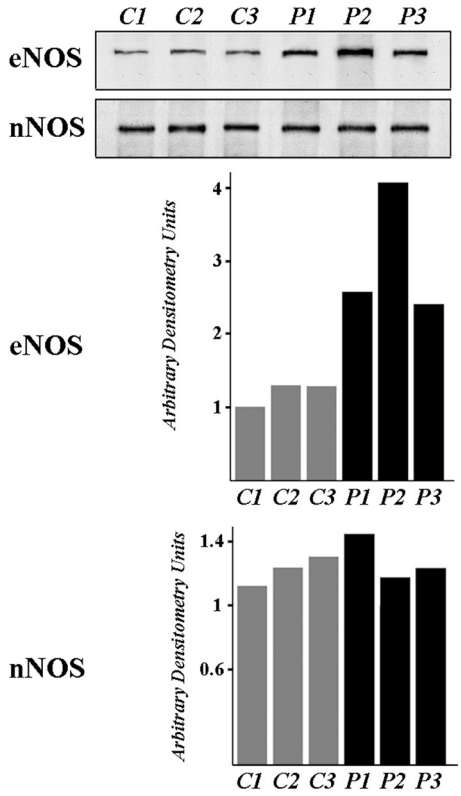


FIG. 5. **Immunoblot analysis of eNOS and nNOS.** Immunoblots demonstrating an increased expression of eNOS in the patients' muscle (*P*) as compared with control muscles (*C*), whereas the expression of nNOS is similar in both patients' and controls' muscles. Densitometric analysis of the stained bands.

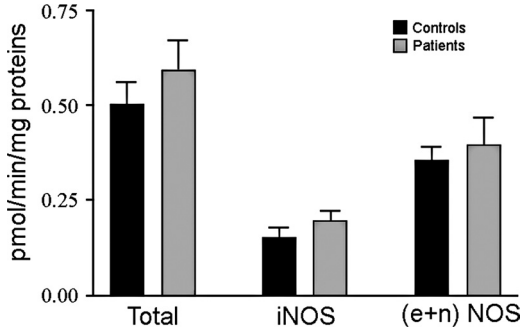


FIG. 6. **Assay of NOS activity.** Box show total NOS activity, the calcium-dependent activity of the constitutive isoforms of NOS (eNOS and nNOS) as well as the calcium-independent activity of iNOS in patients' and in control muscles. The differences between the two groups are not statistically significant. Data are from eight patients with mitochondrial diseases and 11 pair-matched controls.

with matched controls (Fig. 7*A*). The spots that were still present in the blot after reducing treatment with sodium dithionite were considered false positive. The 11 spots specifically observed in MD were identified by mass spectrometry analysis as listed in Table III (see also supplemental Table 1).

Immunoprecipitation of six (vimentin, desmin, ATP synthase $\beta$-chain subunit, protein disulfide-isomerase A3, volt-

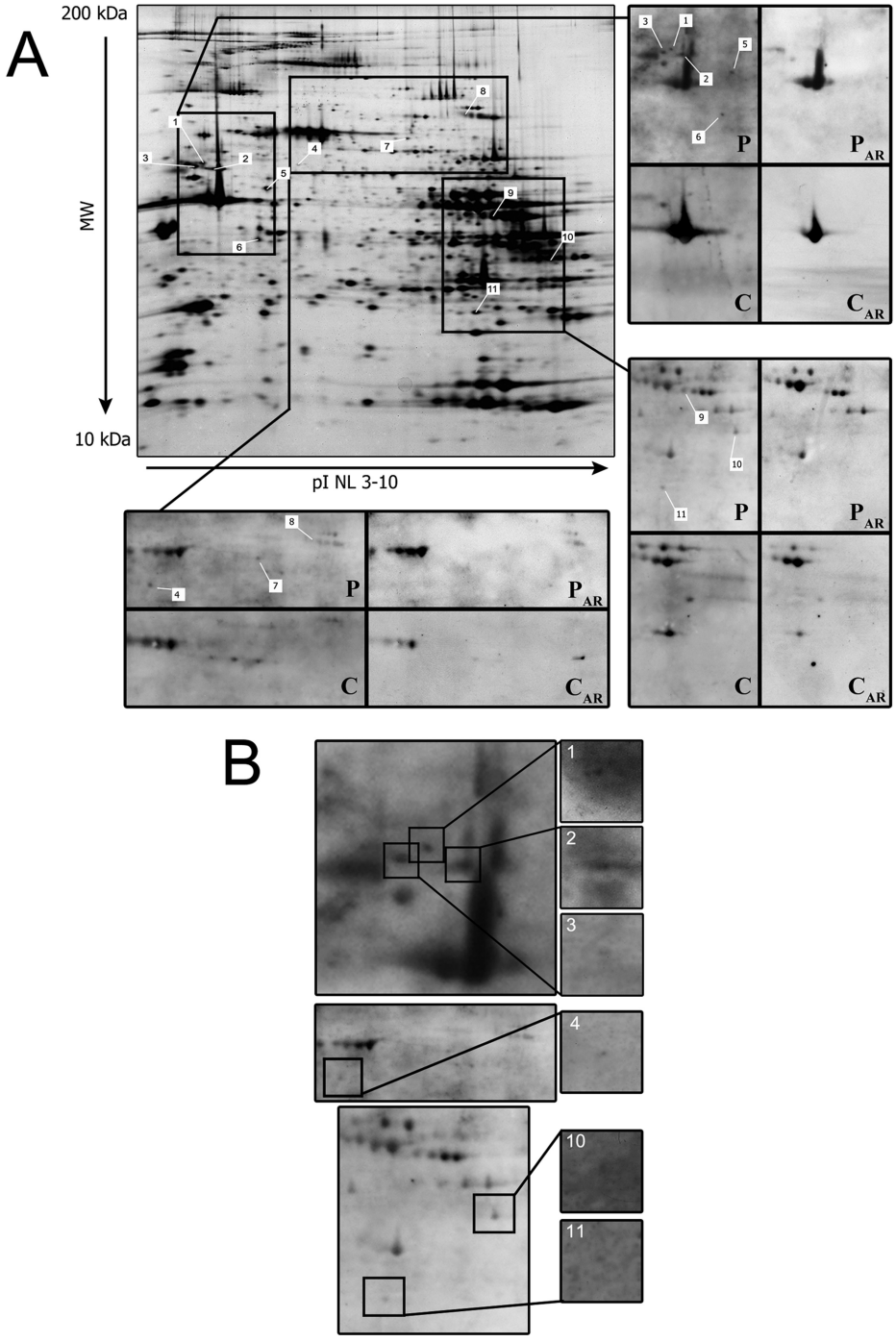


FIG. 7. **Two-dimensional gel silver staining and two-dimensional immunoblotting using antibody to 3-nitrotyrosine.** Immunoprecipition of vimentin, desmin, ATP synthase $\beta$-chain subunit, protein disulfide-isomerase A3, voltage-dependent anion channel 1 and MnSOD and immunoblotting using antibody to 3-nitrotyrosine. *A*-Matching immunoreactive spots specifically present in MD patients are squared and numbered in a representative two-dimensional silver-stained gel and in the corresponding anti-3-nitrotyrosine two-dimensional immunoblotting of a patient (P) and a control (C) before and following reduction (AR). The immunopositive spots detected following the reduction were not considered for further analysis. The corresponding proteins were identified as reported in Table III. *B*-Anti-3-nitrotyrosine two-dimensional immunoblotting following immunoprecipitation of vimentin, desmin, ATP synthase $\beta$-chain subunit, protein disulfide-isomerase A3, voltage-dependent anion channel 1, and MnSOD shows expected spots corresponding to proteins.

age-dependent anion channel 1, and MnSOD) out of the 11 proteins and Western blotting with the antibody to 3-NT revealed expected spots corresponding to the above proteins in MD patients' muscle, but not in the controls' muscle (Fig. 7*B*). These results ensure that the proteins identified by mass spectrometry are indeed the ones nitrated.

*Flow-mediated Vasodilatation and Echo-Doppler Analysis*—A statistically significant difference in FMD (AUC, minutes 0–8) of BA and CFA was observed between patients and controls whereas no differences in endothelium-independent vasodilatation (AUC, minutes 0–5) were present (Fig. 8). The arterial diameters at baseline and the increase in blood flow-velocity were similar in patients and controls, thus indicating that differences were not related to variations of baseline vascular geometry and driving force for endothelium-dependent vasodilatation (Table IV). Blood pressure and heart rate, measured every 2 mins throughout the hemodynamic tests, did not vary significantly within

TABLE III
*The eleven nitrated protein identified in MD patients*

| Protein Function | Spot | Protein | Accession number |
|---|---|---|---|
| ENERGY METABOLISM | 8 | ACONITATE HYDRATASE | Q99798 |
| | 3 | ATP SYNTHASE $\beta$-CHAIN SUBUNIT | P06576 |
| | 6 | PYRUVATE DEHYDROGENASE E1 COMPONENT SUBUNIT BETA | P11177 |
| | 7 | SUCCINATE DEHYDROGENASE [UBIQUINONE] FLAVOPROTEIN SUBUNIT | P31040 |
| | 5 | UBIQUINOL-CYTOCHROME-C REDUCTASE COMPLEX CORE PROTEIN 1 | P31930 |
| | 9 | CREATIN KINASE | P06732 |
| CYTOSKELETAL | 2 | DESMIN | P17661 |
| | 1 | VIMENTIN | P08670 |
| CHAPERONE | 4 | PROTEIN DISULFIDE-ISOMERASE A3 | P30101 |
| ANTIOXIDANT | 11 | MnSOD | Q6LEN1 |
| ION CHANNEL | 10 | VOLTAGE-DEPENDENT ANION CHANNEL 1 | (P21796) |

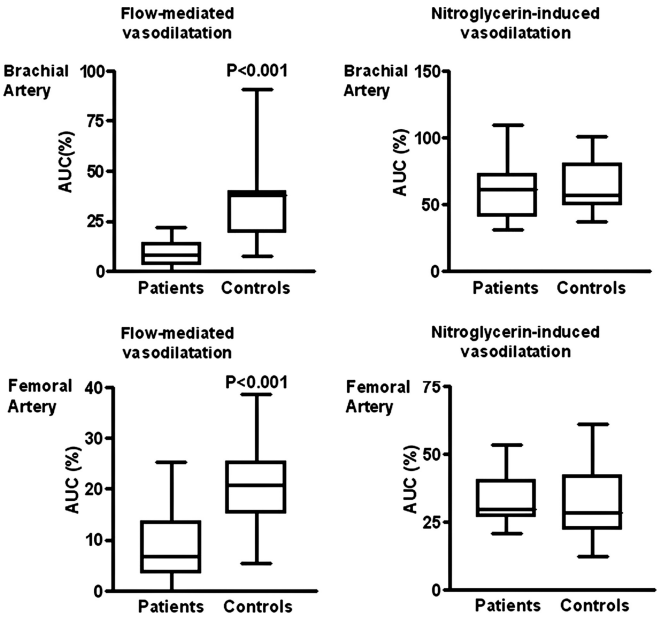


FIG. 8. **Flow-mediated vasodilatation and endothelium-independent vasodilatation of brachial and common femoral artery.** Box and whisker plots show the percentage increase in arterial diameters as a function of time (area under the curve, AUC) induced by distal hyperemia (flow-mediated vasodilatation) and by the sublingual administration of nitroglycerin. Data are from 16 patients with mitochondrial diseases and 16 pair-matched controls.

each subject (data not shown). No differences were observed between patients and controls for the prevalence of carotid artery stenosis or increased intima/media thickness.

## DISCUSSION

The major result from the present study is the recognition of the vessel wall as a target of oxidative and nitrative stress in patients affected with mitochondrial respiratory chain dysfunction. In addition, our data indicate that increased oxidative and nitrative stress may reduce NO bioactivity in the vasculature of MD patients.

We identified 3-NT immunoreactivity in the small blood vessels of MD patients regardless from the clinical phenotype and the genetic mutation, and the amount of 3-NT was

TABLE IV
*Arterial diameters at baseline and increase in blood flow-velocity*

| VARIABLE Median (range) | Subjects with MD ($n$ = 16) | Control Subjects ($n$ = 16) |
|---|---|---|
| Basal arterial diameter (mm) | 4.20 (3.10–5.20) | 4.20 (3.50–5.20) |
| Increase in blood flow velocity (%) | 129 (8–1000) | 156 (15–531) |
| VARIABLE Median (range) | Subjects with MDs ($n$ = 16) | Control Subjects ($n$ = 16) |
| Basal arterial diameter (mm) | 7.50 (5.60–10.20) | 8.20 (5.60–10.90) |
| Increase in blood flow velocity (%) | 178 (-21–1160) | 163 (-6–940) |

significantly higher in the patients' muscle samples as compared with control muscles. The increased 3-NT expression, observed by immunohistochemistry and confocal immunofluorescence microscopy in the muscle biopsies from all the studied patients, was specifically located in the endothelium and smooth muscle cells of the vessel wall.

3-NT results from nitration of free tyrosine or protein tyrosine residues through one of the two relevant nitration pathways that operate *in vivo*, namely peroxynitrite and heme peroxidase-dependent nitration (11, 12). Therefore, 3-NT accumulation reflects a loss of balance between oxidant formation and antioxidant defense mechanisms, known as oxidative and nitrosative stress (22, 23).

After showing the increased levels of nitrotyrosine, we performed a detailed proteomic analysis on muscle biopsy from our MD patients in order to characterize the proteins that undergo a tyrosine nitration. We identified 11 specific proteins that are nitrated under pathological conditions and that can be grouped into classes based on their recognized functions: energy metabolism, cytoskeletal, chaperone, antioxidant, and ion channel (Table II). Interestingly, most of these nitrated proteins are involved in energy metabolism and are mainly located in mitochondria. Mitochondrial proteins appear to be particularly susceptible to nitration mechanisms (24, 25). Recent data indicate that under conditions

of acute oxidative stress the nitration of mitochondrial proteins is a reversible dynamic process, because of a mechanism not yet identified, thus suggesting that nitration might be a cellular signaling mechanism (26, 27).

The identification of several proteins that have an important role in energy metabolism offers, therefore, a potential rationale for the biological dysfunction of blood vessels in MD patients. Tyrosine nitration has been detected in several pathological conditions including neurodegenerative and inflammatory diseases (28). The biological significance of modifying tyrosine residues by nitration is under investigation, with several potential consequences such as alterations in the secondary structure, function, and proteolytic removal, which could deeply modulate the cellular function (13–15). Published data strongly indicate the utility of nitrotyrosine as a potential biological marker to determine risk associations with cardiovascular diseases (29).

After showing the increased levels of nitrotyrosine and the presence of specific nitratred proteins in MDs, we addressed the relevance of nitric oxide synthase enzymes in the production of nitric oxide (NO). NO generation is catalyzed by three distinct isoforms of nitric oxide synthase (NOS) (30). Two isoforms are constitutively expressed, one in endothelial cells (eNOS) and the other in the brain (nNOS) and both are calcium-dependent; the third isoform, inducible (iNOS), is regulated primarily at the transcriptional level and is calcium-independent (30). Via immunoblot analysis we documented an up-regulation of eNOS in muscle biopsies of MD patients and by confocal immunofluorescence microscopy we demonstrated its location specifically in the vessel wall. The distribution of eNOS-positive immunostaining was similar in patients and controls. The image analysis of eNOS-positive blood vessels, performed in muscle biopsy from seven controls and seven MD patients with clinical heterogeneous presentation using the NIH Scion Image analysis program, showed that eNOS-positive area was significantly higher in the patients. These data confirm the increased expression of the protein as demonstrated by immunoblot and support the view that an overactivation of eNOS could occur and be responsible for the increased levels of nitric oxide. Unlike eNOS, we did not detect in blood vessels any significant abnormal immunoreactivity of the other two isoforms of NOS including nNOS and iNOS; nNOS expression was similar in the patients' and in controls' muscle thus suggesting that these enzymes are not casually involved in the production of nitrating species. Unfortunately, the data on quantitative measurement of eNOS activity are not so straightforward. The increased activity of the total and of the constitutive isoforms of NOS in MD patients' muscle was not statistically significant in contrast with the clear demonstration of an increased expression. This discrepancy may be because of the biochemical assay that does not distinguish the activities of the two constitutive isoforms of NOS. Alternatively, the uncoupling of eNOS resulting from the oxidative and nitrative stress could lead to a significant impairment of NO production which, in turn, could concur to injure the flow mediated vasodilatation.

Once we proved that in MDs the vessel walls are involved in oxidative and nitrative stress, we evaluated the endothelial function *in vivo* by measuring FMD in the same MD patients. This noninvasive functional test has been used to investigate the release and bioactivity of NO in the peripheral vasculature, because vasodilatation is specifically prevented by the administration of endothelial NO synthase inhibitors (31).

The reduced FMD observed in these patients is accompanied by a preserved vasodilatatory response to the sublingual administration of nitroglycerin, thus indicating that structural changes in the vascular wall or reduced relaxant capacity of smooth muscle cells are unlikely responsible for the altered vascular response. Therefore, we hypothesize that the decreased NO bioactivity, because of the formation of reactive nitrogen species, provide an adequate explanation of our findings and the nitrotyrosine accumulation in the blood vessels of these MD patients strongly sustains this view (11, 12).

The increased oxidative and nitrative stress and the modified vascular function in MD may be of relevance for the pathophysiology of these disorders and may also give clues for the understanding of the biochemical mechanism implicated in endothelial dysfunction. A blunted or absent increase in shear stress and NO-induced vasodilatation in peripheral arteries may result in increased vascular resistance and inadequate blood supply, further worsening the energetic imbalance in skeletal muscle because of ineffective ATP generation. Recent data from experimental models indicate that mitochondrial dysfunction is associated with cardiovascular alterations including increased blood pressure, atherosclerosis, and premature aging (32, 33). Moreover, mtDNA mutations have been associated with increased blood pressure also in humans (34–37). The accumulation of nitrotyrosine, not only within the vascular wall of MD patients, but also, to some extent, in the small vessels from all, but the youngest control subjects, suggests that mitochondrial dysfunction may anticipate the unavoidable fate of age- and oxidation-related dysfunctional endothelium that is observed in the general population and in experimental models (13, 38, 39).

S This article contains supplemental Table S1.

‡‡ To whom correspondence should be addressed: Department of Neurological Sciences and Vision, Section of Clinical Neurology, Policlinico G.B. Rossi, P.le L.A. Scuro 10, 37134 Verona. Phone: +39-045-8124461; Fax: +39-045-585933; E-mail: giuliano.tomelleri@univr.it.

REFERENCES

1. DiMauro, S., and Schon, E. A. (2003) Mitochondrial respiratory-chain diseases. *N. Engl. J. Med.* **348,** 2656–2668
2. McKenzie, M., Liolitsa, D., and Hanna, M. G. (2004) Mitochondrial disease: mutations and mechanisms. *Neurochem. Res.* **29,** 589–600

3. Zeviani, M., and Di Donato, S. (2004) Mitochondrial disorders. *Brain* **127,** 2153–2172
4. Gerbitz, K. D., van den Ouweland, J. M., Maassen, J. A., and Jaksch, M. (1995) Mitochondrial diabetes mellitus: a review. *Biochim. Biophys. Acta* **1271,** 253–260
5. Filosto, M., Tonin, P., Vattemi, G., Spagnolo, M., Rizzuto, N., and Tomelleri, G. (2002) Antioxidant agents have a different expression pattern in muscle fibers of patients with mitochondrial disease. *Acta Neuropathol.* **103,** 215–220
6. Pitkanen, S., and Robinson, B. H. (1996) Mitochondrial complex I deficiency leads to increased production of superoxide radicals and induction of superoxide dismutase. *J. Clin. Invest.* **98,** 345–351
7. Dröge, W. (2002) Free radicals in the physiological control of cell function. *Physiol. Rev.* **82,** 47–95
8. Gryglewski, R. J., Palmer, R. M., and Moncada, S. (1986) Superoxide anion is involved in the breakdown of endothelium-derived vascular relaxing factor. *Nature* **320,** 454–456
9. Loscalzo, J. (1995) Nitric oxide and vascular disease. *N. Engl. J. Med.* **333,** 251–253
10. Iadecola, C., Pellegrino, D. A., Moskowitz, M. A., and Lassen, N. A. (1994) Nitric oxide synthase inhibition and cerebrovascular regulation. *J. Cereb. Blood Flow Metab.* **14,** 175–92
11. Crow, J. P., and Beckman, J. S. (1995) Reactions between nitric oxide, superoxide, and peroxynitrite: footprints of peroxynitrite in vivo. *Adv. Pharmacol.* **34,** 17–43
12. Beckman, J. S., and Koppenol, W. H. (1996) Nitric oxide, superoxide, and peroxynitrite: the good, the bad, and ugly. *Am. J. Physiol.* **271,** C1424–37
13. Greenacre, S. A., and Ischiropoulos, H. (2001) Tyrosine nitration: localisation, quantification, consequences for protein function and signal transduction. *Free Radic. Res.* **34,** 541–581
14. Kanski, J., and Schöneich, C. (2005) Protein nitration in biological aging: proteomic and tandem mass spectrometric characterization of nitrated sites. *Methods Enzymol.* **396,** 160–171
15. Ischiropoulos, H. (2003) Biological selectivity and functional aspects of protein tyrosine nitration. *Biochem. Biophys. Res. Commun.* **305,** 776–783
16. DiMauro, S., Moraes, C. T. (1993) Mitochondrial encephalomyopathies. *Arch. Neurol.* **50,** 1197–1208
17. Vattemi, G., Tonin, P., Mora, M., Filosto, M., Morandi, L., Savio, C., Dal, Pra, I., Rizzuto, N., and Tomelleri, G. (2004) Expression of protein kinase C isoforms and interleukin-1beta in myofibrillar myopathy. *Neurology* **62,** 1778–1782
18. Miyagi, M. Sakaguchi, H., Darrow, R. M., Yan, L., West, K. A., Aulak, K. S., Stuehr, D. J., Hollyfield, J. G., Organisciak, D. T., and Crabb, J. W. (2002) Evidence that light modulates protein nitration in rat retina. *Mol. Cell. Proteomics* **1,** 293–303
19. Klouckova, I., Hrncirova, P., Mechref, Y., Arnold, R. J., Li, T. K., McBride, W. J., and Novotny, M. V. (2006) Changes in liver protein abundance in inbred alcohol-preferring rats because of chronic alcohol exposure measured through a proteomics approach. *Proteomics* **6,** 3060–3074
20. Mann, B., Madera, M., Sheng, Q., Tang, H., Mechref, Y., and Novotny, M. V. (2008) ProteinQuant Suite: a bundle of automated software tools for label-free quantitative proteomics. *Rapid Commun. Mass Spectrom.* **22,** 3823–3834
21. Arcaro, G., Cretti, A., Balzano, S., Lechi, A., Muggeo, M., Bonora, E., and Bonadonna, R. C. (2002) Insulin causes endothelial dysfunction in humans: sites and mechanisms. *Circulation* **105,** 576–582
22. Sies, H. (1991) Oxidative stress: from basic research to clinical application. *Am. J. Med.* **91,** 31S-38S
23. Radi, R., Peluffo, G., Alvarez, M. N., Naviliat, M., and Cayota, A. (2001) Unraveling peroxynitrite formation in biological systems. *Free Radic. Biol. Med.* **30,** 463–488
24. Elfering, S. L., Haynes, V. L., Traaseth, N. J., Ettl, A., and Giulivi, C. (2004) Aspects, mechanism, and biological relevance of mitochondrial protein nitration sustained by mitochondrial nitric oxide synthase. *Am. J. Physiol. Heart Circ. Physiol.* **286,** H22-H29
25. Turko, I. V., Li, L., Aulak, K. S., Stuehr, D. J., Chang, J. Y., and Murad, F. (2003) Protein tyrosine nitration in the mitochondria from diabetic mouse heart. Implications to dysfunctional mitochondria in diabetes. *J. Biol. Chem.* **278,** 33972–33977
26. Aulak, K. S., Koeck, T., Crabb, J. W., and Stuehr, D. J. (2004) Dynamics of protein nitration in cells and mitochondria. *Am. J. Physiol. Heart Circ. Physiol.* **286,** H30-H38
27. Koeck, T., Fu, X., Hazen, S. L., Crabb, J. W., Stuehr, D. J., and Aulak, K. S. (2004) Rapid and selective oxygen-regulated protein tyrosine denitration and nitration in mitochondria. *J. Biol. Chem.* **279,** 27257–27262
28. Pacher, P., Beckman, J. S., and Liaudet, L. (2007) Nitric oxide and peroxynitrite in health and disease. *Physiol. Rev.* **87,** 315–424
29. Shishehbor, M. H., Aviles, R. J., Brennan, M. L., Fu, X., Goormastic, M., Pearce, G. L., Gokce, N., Keaney, J. F., Jr., Penn, M. S., Sprecher, D. L., Vita, J. A., and Hazen, S. L. (2003) Association of nitrotyrosine levels with cardiovascular disease and modulation by statin therapy. *JAMA* **289,** 1675–1680
30. Bian, K., Ke, Y., Kamisaki, Y., and Murad, F. (2006) Proteomic modification by nitric oxide. *J. Pharmacol. Sci.* **101,** 271–279
31. Joannides, R., Richard, V., Haefeli, W. E., Benoist, A., Linder, L., Lüscher, T. F., and Thuillez, C. (1997) Role of nitric oxide in the regulation of the mechanical properties of peripheral conduit arteries in humans. *Hypertension* **30,** 1465–1470
32. Bernal-Mizrachi, C., Gates, A. C., Weng, S., Imamura, T., Knutsen, R. H., DeSantis, P., Coleman, T., Townsend, R. R., Muglia, L. J., and Semenkovich, C. F. (2005) Vascular respiratory uncoupling increases blood pressure and atherosclerosis. *Nature* **435,** 502–506
33. Trifunovic, A., Wredenberg, A., Falkenberg, M., Spelbrink, J. N., Rovio, A. T., Bruder, C. E., Bohlooly-Y, M., Gidlöf, S., Oldfors, A., Wibom, R., Törnell, J., Jacobs, H. T., and Larsson, N. G. (2004) Premature ageing in mice expressing defective mitochondrial DNA polymerase. *Nature* **429,** 417–423
34. Austin, S. A., Vriesendorp, F. J., Thandroyen, F. T., Hecht, J. T., Jones, O. T., and Johns, D. R. (1998) Expanding the phenotype of the 8344 transfer RNAlysine mitochondrial DNA mutation. *Neurology* **51,** 1447–1450
35. Watson, B., Jr., Khan, M. A., Desmond, R. A., and Bergman, S. (2001) Mitochondrial DNA mutations in black Americans with hypertension-associated end-stage renal disease. *Am. J. Kidney Dis.* **38,** 529–536
36. Schwartz, F., Duka, A., Sun, F., Cui, J., Manolis, A., and Gavras, H. (2004) Mitochondrial genome mutations in hypertensive individuals. *Am. J. Hypertens.* **17,** 629–635
37. Wilson, F. H., Hariri, A., Farhi, A., Zhao, H., Petersen, K. F., Toka, H. R., Nelson-Williams, C., Raja, K. M., Kashgarian, M., Shulman, G. I., Scheinman, S. J., and Lifton, R. P. (2004) A cluster of metabolic defects caused by mutation in a mitochondrial tRNA. *Science* **306,** 1190–1194
38. Celermajer, D. S., Sorensen, K. E., Spiegelhalter, D. J., Georgakopoulos, D., Robinson, J., and Deanfield, J. E. (1994) Aging is associated with endothelial dysfunction in healthy men years before the age-related decline in women. *J. Am. Coll. Cardiol.* **24,** 471–476
39. Csiszar, A., Ungvari, Z., Edwards, J. G., Kaminski, P., Wolin, M. S., Koller, A., and Kaley, G. (2002) Aging-induced phenotypic changes and oxidative stress impair coronary arteriolar function. *Circ. Res.* **90,** 1159–1166